Metallophysics and Advanced Technologies
Металофіз. новітні технол.
Metallofiz. Noveishie Tekhnol.
2022, vol. 44, No. 7, pp. 913–926
https://doi.org/10.15407/mfint.44.07.0913
Reprints available directly from the publisher

PACS numbers: 61.66.Dk, 61.72.Yx, 64.75.-g, 68.43.Mn, 82.30.Rs, 82.80.-d

Structure, Phase Composition and Hydrogen Absorption Properties of Multiphase Alloys of Ti–Zr–Mn–V System Alloyed with Holmium

V. A. Dekhtyarenko, T. V. Pryadko, D. G. Savvakin, and V. I. Bondarchuk

G. V. Kurdyumov Institute for Metal Physics, N.A.S. of Ukraine,
36 Academician Vernadsky Blvd.,
UA-03142 Kyiv, Ukraine

The effect of an RE element (holmium) on the phase composition, microstructure, and hydrogen absorption properties of multiphase alloys of the Ti–Zr–Mn–V system comprised of the Laves phase and b.c.c. solid solution is studied. It is found out that holmium practically does not dissolve in the initial phases of the alloy, and it forms a new phase in combination with oxygen, holmium oxide. The crystallites of holmium oxide precipitate on the surface of the crystallites of the Laves phase and b.c.c. solid solution. It is determined that the formation of the new phase leads to a change in the structure of the initial alloys from eutectic to multiphase, that causes an increase in the grain surface area of the phase constituents. It is shown that the crystallites of holmium oxide raise the temperatures at which hydrogen absorption and desorption occur, as well as decrease the hydrogen capacity of the alloy.

Key words: Laves phase, b.c.c. solid solution, multiphase alloy, microstructure, phase composition, hydrogenation.

Досліджено вплив леґування РЗМ (Гольмій) на фазовий склад, мікроструктуру та водневосорбційні властивості гетерофазних стопів системи Ti–Zr–Mn–V зі структурою фази Лавеса та ОЦК-твердого розчину. Встановлено, що введений в стоп Гольмій, практично не розчиняється у вихідних фазах, а з'єднавшись з Оксиґеном, утворює нову фазу, оксид Гольмію. Утворені кристали оксиду Гольмію розміщуються виключно по поверхні кристалів інтерметаліду. Визначено, що утворення нової фази приводить

Corresponding author: Volodymyr Anatoliyovych Dekhtyarenko
E-mail: Devova@i.ua

Citation: V. A. Dekhtyarenko, T. V. Pryadko, D. G. Savvakin, and V. I. Bondarchuk, Structure, Phase Composition, and Hydrogen Absorption Properties of Multiphase Alloys of Ti–Zr–Mn–V System Alloyed with Holmium, *Metallofiz. Noveishie Tekhnol.*, **44**, No. 7: 913–926 (2022). DOI: 10.15407/mfint.44.07.0913

до зміни структури стопів від евтектичної до гетерофазної, зі збільшенням площі поверхні зерен співіснуючих фаз на порядок. Показано, що присутність у фазовому складі стопу кристалів оксиду Гольмію приводить до погіршення процесів поглинання та виділення Гідроґену, а також до пониження водневої місткости стопу.

Ключові слова: фаза Лавеса, ОЦК-твердий розчин, гетерофазні стопи, мікроструктура, фазовий склад, гідрування.

(Received May 4, 2022; in final version, May 19, 2022)

1. INTRODUCTION

It has now been shown that storing hydrogen in a bound state (metal hydrides) is a more cost-effective and safe way than in liquid or gaseous states [1–5]. Among the existing variety of materials for hydrogen sorption, the AB_2-type intermetallics (hexagonal Laves phase of $C14$ type) and multiphase alloys based on them are recently used, especially in transport [6–10]. In this class of materials, an important place is occupied by the Ti-based alloys. Therefore, the increasing requirements for these materials demand the development and production of new alloys based on this type of compounds. Based on the previous data [11–13], several researchers have shown that the improvement of the kinetics of sorption–desorption processes and significant increase of the amount of absorbed hydrogen in the alloys based on the Laves phase can be achieved only by additional alloying of this phase [14–16].

The hydrogen absorption properties of a single-phase alloy comprised of hexagonal $C14$-type Laves phase additionally alloyed with nickel, cobalt, or copper were studied in [17], and the relationship between the change of the unit cell volume and the amount of absorbed hydrogen was found out. The authors noted that the crystal lattice parameters gradually increased in the sequence of alloying elements $\mathrm{Ni} \rightarrow \mathrm{Fe} \rightarrow \mathrm{Cu}$, so the unit cell volume changed from 165.591 to 166.771 Å^3. The increase in the unit cell volume when replacing nickel with copper was explained in [17], according to the data of [18], by the different atomic radii of these elements (0.125 nm and 0.128 nm, respectively), while the amount of all other components was constant. The increment in the unit cell volume of the alloys in the $\mathrm{Ni} \rightarrow \mathrm{Fe} \rightarrow \mathrm{Cu}$ sequence led to an increase in the amount of absorbed hydrogen in a range of 1.79–1.81% wt. [17].

The effect of adding RE elements (La, Ce, Ho) into the alloys based on the $C14$ type Laves phase on their hydrogen absorption properties was investigated in [19]. These elements were chosen due to their ability to interact with hydrogen and form a hydride phase. The authors of [19] claim that the alloying with RE elements enhances the hydrogenation kinetics. In contrast to the original composition, the same alloys with RE elements can absorb hydrogen at room temperature. However, the

data on the possible changes in the amount of hydrogen absorbed by the alloys after adding RE elements were not provided.

Our previous studies [20, 21] of multiphase alloys of the Ti–Zr–Mn–V and Ti–Zr–Mn–V–Cr systems confirmed that adding the elements with a larger atomic radius, which can form stable chemical compounds with hydrogen, usually leads to enhanced hydrogen absorption. Nevertheless, it is necessary to take into account other factors that can limit this pattern. An analysis of the literature [22–26] showed that most researchers have used for Ti-based alloys with a Laves phase structure, or multiphase alloys comprised of AB_2-type intermetallic phase and b.c.c. solid solution, the elements from the same period (zirconium and hafnium) or group (from vanadium to nickel) of titanium in the periodic table. However, these elements, except zirconium, vanadium, and chromium, have low affinity for hydrogen or do not react with it at all [10]. In addition, the elements of the same group with titanium with higher atomic number have smaller atomic radii [18]. Therefore, to clarify the above mentioned pattern, additional alloying was necessary to choose an element with a significantly larger atomic radius compared to other components of the alloy, that could efficiently interact with hydrogen. The RE metals met these requirements.

In this work, holmium was chosen to verify the effect of alloying by RE elements on the hydrogen adsorption properties of multiphase alloys of the Ti–Zr–Mn–V system. According to [19], La, Ce, and Ho affect the hydrogen absorption properties of the Ti–Zr–Mn–V alloys almost in the same way. Despite the fact that holmium (Ho) has the smallest atomic radius among these RE elements (atomic radii of Ho and La are 0.179 and 0.187 nm, respectively [18]), it meets all the conditions that are needed to increase the hydrogen capacity of the alloy: its atomic radius is larger compared to other components of the Ti–Zr–Mn–V system (0.160 nm for zirconium and lower for other elements), and holmium can form with hydrogen a chemical compound HoH_3. To clarify the effect of holmium addition, the previously studied alloys of hypoeutectic $Ti_{47.5}Zr_{30}Mn_{17.5}V_5$ [20, 27] and hypereutectic $Ti_{44.18}Zr_{27.9}Mn_{20.93}V_7$ [28] compositions were selected. The studies were carried out by comparing the structure, phase composition and hydrogen adsorption properties of the alloys (Table 1) with those without holmium ($Ti0_{47.5}Zr_{30}Mn_{17.5}V_5$ and $Ti_{44.18}Zr_{27.9}Mn_{20.93}V_7$) as a reference which were studied in detail in [27, 28]. According to [27, 28], there were eutectic component and primary crystallites in the both alloys without holmium. There were primary crystallites of the b.c.c. solid solution in the $Ti_{47.5}Zr_{30}Mn_{17.5}V_5$ alloy, while the $Ti_{44.18}Zr_{27.9}Mn_{20.93}V_7$ alloy contained the Laves phase. The range of holmium content was chosen the same as for the multiphase alloys of the Ti–Zr–Mn–V system [20, 21], *i.e.,* 2 and 5 at.% (Table 1). Holmium replaced only manganese, and so it increased the total amount of hydride-forming constituent in the alloy (Table 1, alloys 1, 2); in order to maximize the unit cell volume, all

TABLE 1. Nominal composition of the alloys.

Alloy No.	Composition									
	at.%					% wt.				
	Ti	Zr	Mn	V	Ho	Ti	Zr	Mn	V	Ho
1	47.5	30	15.5	5	2	35.28	42.45	13.20	3.95	5.12
2	47.5	30	12.5	5	5	33.56	40.38	10.13	3.76	12.17
3	43.29	27.34	20.51	6.86	2	32.52	39.14	17.68	5.48	5.18
4	41.97	26.50	19.88	6.65	5	30.07	36.18	16.34	5.07	12.34

components were replaced (Table 1, alloys 3, 4).

2. MATERIALS AND EXPERIMENTAL PROCEDURE

The alloys were manufactured by arc melting in argon atmosphere. Ingots of 30 g were produced using iodide titanium (of 99.95% purity), iodide zirconium (99.975%), electrolytic vanadium (99.9%), electrolytic manganese (99.9%) and holmium (99.9%) as raw materials. The ingots were remelted 4–5 times to achieve sufficient uniformity.

The interaction of the alloys with hydrogen was studied by the Sieverts method at an IVGM-2M unit [29] under mild conditions (room temperature, absolute pressure ~ 0.6 MPa), as well as upon continuous heating up to 550°C (heating rate 0.125°C/s) and during isothermal exposure at selected temperature under the same hydrogen pressure. The alloys in as-cast state were studied; cylindrical specimens with a diameter of 11–12 mm and a height of 4–5 mm were used. The amount of absorbed hydrogen was calculated from the change in pressure in a closed volume, and was also determined by weighing samples on VLR 20 scales with an accuracy of $1.5 \cdot 10^{-5}$ g. The investigation included only one hydrogenation cycle in order to determine the effect of holmium on the first hydrogenation in the Ti–Zr–Mn–V–Ho alloys.

The phase composition and parameters of crystalline lattices of the alloy before and after hydrogenation were determined by x-ray phase analysis. Metallographic examinations were performed with a scanning electron microscope VEGA3 TESCAN equipped with EDX detector XFlash610M (Bruker).

3. RESULTS AND DISCUSSION

3.1. Structure and Phase Composition

The microstructures of the alloys are shown in Fig. 1. As seen, the

addition of holmium into the eutectic alloys of the Ti–Zr–Mn–V system, regardless of its amount and the elements it replaced, resulted in significant microstructural changes. After adding holmium (regardless of its concentration), the microstructure of the alloy changed from two-phase (eutectic) (Fig. 1, *a*) to three-phase (Fig. 1, *b*–*e*), with a significant change in the morphology of the phase constituents.

In order to distinguish the phases and to determine their chemical composition, the alloys were investigated using local energy-dispersion analysis (Table 2).

Based on the above data (Table 2), it can be suggested that holmium is practically insoluble in the phase components of the initial alloys, and in combination with oxygen it forms a separate phase, holmium oxide (white crystallites, Figs. 1, *b*–*e*). According to the chemical composition of the crystallites (in particular, the manganese concentration), the bright-grey phase is intermetallic, and the dark-grey one is Ti-based b.c.c. solid solution.

On the example of the $Ti_{47.5}Zr_{30}Mn_{12.5}V_5Ho_5$ alloy microstructure (Fig. 1, *c*), it is seen that the crystallites of holmium oxide are located at the grain boundaries. It can be assumed that the segregation of holmium oxide occurred during solidification, and then a gradual saturation of holmium with oxygen by diffusion in the solid state with a gradual

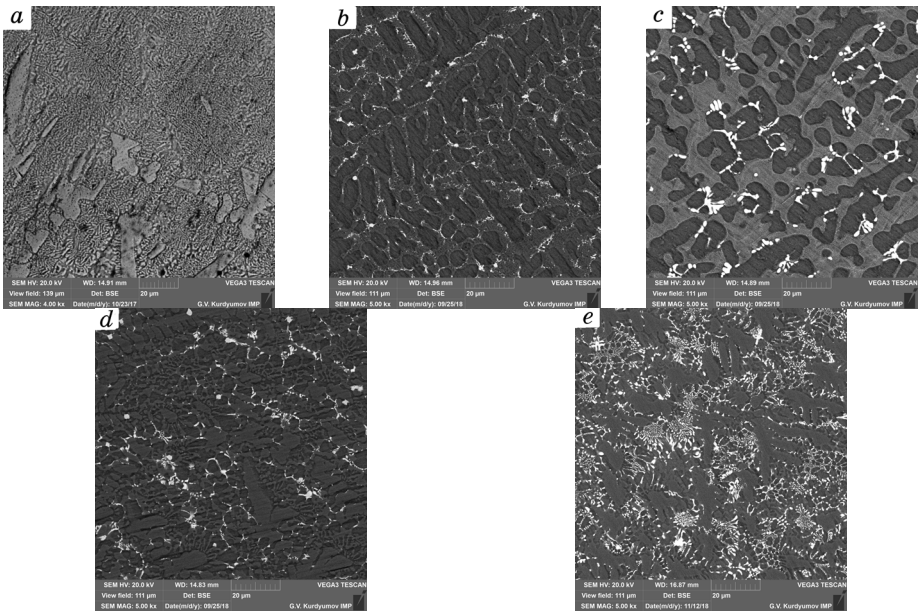

Fig. 1. Microstructure of cast alloys: $Ti_{44.18}Zr_{27.9}Mn_{20.93}V_7$ [28] (*a*), $Ti_{47.5}Zr_{30}Mn_{17.5}V_5Ho_2$ (*b*), $Ti_{47.5}Zr_{30}Mn_{12.5}V_5Ho_5$ (*c*), $Ti_{42.39}Zr_{27.34}Mn_{20.51}V_{6.86}Ho_2$ (*d*), $Ti_{41.97}Zr_{26.5}Mn_{19.88}V_{6.65}Ho_5$ (*e*).

TABLE 2. Chemical composition of the phases.

Alloy No.	Chemical composition (± 0.03 at.%)											
	Bright grey areas					Dark grey areas					White areas	
	Ti	Zr	Mn	V	Ho	Ti	Zr	Mn	V	Ho	Ho	O
1	45.84	27.57	21.18	5.29	0.12	63.71	29.50	4.49	1.96	0.34	62.49	34.96
2	42.08	27.57	23.38	6.45	0.52	62.56	29.25	4.95	2.63	0.61	63.04	36.96
[27] (initial)	32.10	18.90	42.00	7.00	–	56.70	36.70	2.80	3.80	–	–	–
3	31.76	23.41	33.35	11.37	0.11	64.87	28.20	4.62	1.93	0.38	63.52	36.48
4	32.04	23.05	33.09	11.35	0.47	64.38	27.71	4.54	2.71	0.66	63.75	36.25
[28] (initial)	28.85	25.88	34.95	10.32	–	68.71	26.41	3.36	1.52	–	–	–

formation of the oxide phase took place.

To confirm the data obtained by scanning electron microscopy and energy-dispersion analysis, the phase composition of the alloys was determined by XRD method (Fig. 2, Table 3). It was found that all the alloys (Table 1), regardless of their chemical composition, still comprised the *C*14-type Laves phase and b.c.c. solid solution, and additionally holmium oxide Ho_2O_3 was detected, as well as some traces of pure holmium.

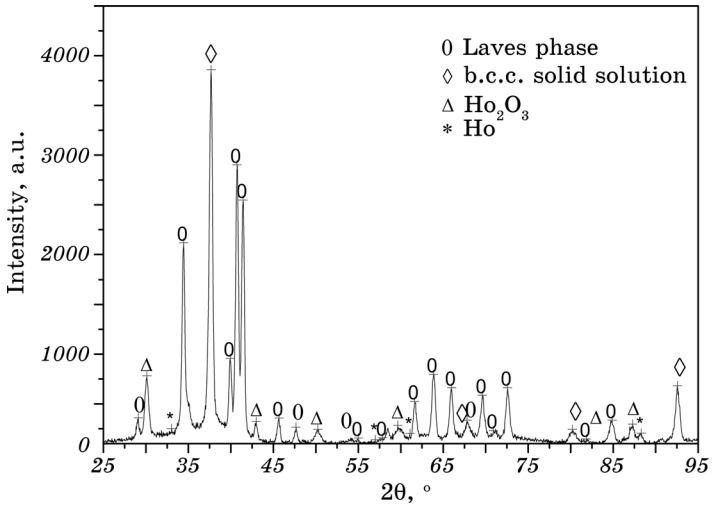

Fig. 2. Diffractogram of cast $Ti_{47.5}Zr_{30}Mn_{15.5}V_5Ho_2$ alloy.

TABLE 3. Lattice parameters of the phases.

Alloy No.	Lattice parameters (± 0.0009 nm)							
	As-cast				Hydrogenated			
	λ-phase	β-phase	Ho_2O_3	Ho	λ-phase	δ-phase	Ho_2O_3	HoH_3
1	$a = 0.5194$ $c = 0.8533$	$a = 0.3375$	$a = 1.0270$	$a = 0.3575$ $c = 0.5649$	$a = 0.5575$ $c = 0.9157$	$a = 0.4585$	$a = 1.0571$	$a = 0.6307$ $c = 0.6559$
2	$a = 0.5193$ $c = 0.8530$	$a = 0.3374$	$a = 1.0256$	$a = 0.3565$ $c = 0.5633$	$a = 0.5578$ $c = 0.9162$	$a = 0.4596$	$a = 1.0549$	$a = 0.6306$ $c = 0.6558$
[27] (initial)	$a = 0.5186$ $c = 0.8528$	$a = 0.3366$	–	–	$a = 0.5574$ $c = 0.9155$	$a = 0.4588$	–	–
3	$a = 0.5185$ $c = 0.8517$	$a = 0.3374$	$a = 1.0260$	$a = 0.3569$ $c = 0.5638$	$a = 0.5576$ $c = 0.9159$	$a = 0.4579$	$a = 1.0572$	$a = 0.6306$ $c = 0.6558$
4	$a = 0.5182$ $c = 0.8513$	$a = 0.3373$	$a = 1.0266$	$a = 0.3567$ $c = 0.5636$	$a = 0.5570$ $c = 0.9150$	$a = 0.4580$	$a = 1.0535$	$a = 0.6303$ $c = 0.6555$
[28] (initial)	$a = 0.5189$ $c = 0.8523$	$a = 0.3357$	–	–	$a = 0.5585$ $c = 0.9150$	$a = 0.4574$	–	–

The volume fractions of the phases were determined by Rietveld analysis; the surface areas of the crystallites of the phase constituents were measured with free distributed ImageJ software. In the alloys 1 and 2, the amounts of holmium oxide, Laves phase, and b.c.c. solid solution equalled 7.74–10.68, 45.45–41.90, and 46.81–47.42%, respectively (Table 1); the surface area of individual grains of the phases was 80–300 μm^2. In alloys 3 and 4, the amounts of holmium oxide and Laves phase equalled 7.85–10.83 and 73.24–70.50%, respectively, and the surface area of their individual grains was 200–300 μm^2; the amount of b.c.c. solid solution was 18.91–18.67%.

It was important to know what changes occurred in the volume of the Laves phase crystal lattice as a result holmium adding, to be able to determine its effect on the total amount of absorbed hydrogen. Besides, according to the data of [30, 31], one can suggest that it is also possible to calculate the radius of the tetrahedral internode in the Laves phase lattice. The approximation of hard spheres is applied, and the expression $Rs(C14) = 0.074475a$ (where a is the lattice parameter) is used only for one type of internodes A_2B_2—it was noted in [30, 31] that dissolved hydrogen occupies exactly them. Comparison of the volume of the unit cell and the radius of the tetrahedral internode (A_2B_2) of the Laves phase for the base composition (without holmium) and alloys with holmium (Fig. 3) shows that Ho addition did not lead to significant changes, despite the atomic radius of holmium (0.179 nm, [18]) is larger than the atomic radii of other components. This result is explained by the fact that holmium is practically insoluble in the Laves phase and b.c.c. solid

solution, and in combination with oxygen it forms a new phase. The increase in the volume of the unit cell of the Laves phase in alloys 1 and 2 in comparison with the base composition $Ti_{47.5}Zr_{30}Mn_{17.5}V_5$ [27] (Fig. 3) was caused by a significant decrease in the Mn amount in this phase (Table 2).

It is also worthwhile to note that according to the JCPDS (International Center for Diffraction Data) the lattice parameter of holmium oxide of stoichiometric composition Ho_2O_3 is 1.0606 nm. However, given the measured values of chemical composition and lattice parameter (1.0256–1.0270 nm) of holmium oxide, as well as the presence of traces of pure holmium which did not interact with oxygen, it can be suggested that oxygen content in the alloy was not high enough to achieve the stoichiometric composition of the oxide.

3.2. The process of Hydrogen Sorption–Desorption

The interaction of the materials with hydrogen was started at room temperature. The coarse crystallites of Laves phase in multiphase alloys of the Ti–Zr–Mn–V system are known to promote the interaction of the material with hydrogen at room temperature [32, 33]. Therefore, active hydrogenation of the alloys with holmium (Table 1) was expected, as they had much larger surface area of Laves phase crystallites (80–300 μm^2) compared to the base alloys (2–8 μm^2) [20, 28]. The alloys of the Ti–Zr–Mn–V–Ho system, as well as the base alloys [20, 28], were exposed at room temperature and an absolute hydrogen pressure of 0.6 MPa for 24–48 hours; however, this did not lead to surface activation and to the expected active hydrogen absorption.

To determine the temperature of active hydrogenation of alloys of the Ti–Zr–Mn–V–Ho system, they were heated in a hydrogen atmosphere up to 450–550°C at a rate of 4–5°C/min and at a constant pressure of 0.6 MPa.

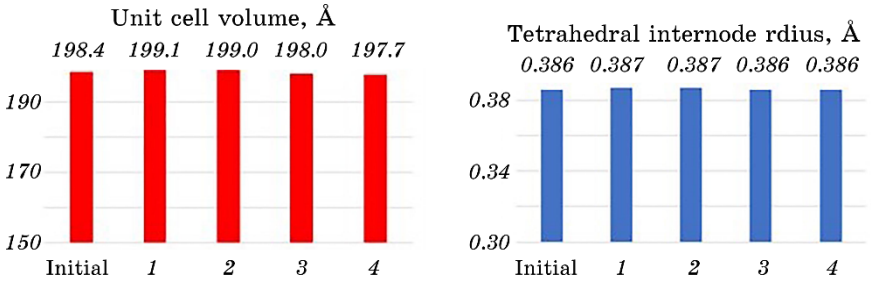

Fig. 3. Unit cell volume and tetrahedral internode radius (A_2B_2) of *C*14 type Laves phase in the studied alloys.

According to the literature [20, 28], the alloys without holmium in the first hydrogenation actively absorb hydrogen at 450°C; the amounts of hydrogen absorbed after isothermal exposure H/Me were ~ 1.81 and 1.70 for the alloys $Ti_{47.5}Zr_{30}Mn_{17.5}V_5$ and $Ti_{44.18}Zr_{27.9}Mn_{20.93}V_7$, respectively (Fig. 4, *a*, *b*). In contrast, the isothermal exposure of Ti–Zr–Mn–V–Ho alloys at 450°C for 1 hour did not result in hydrogen absorption. In the alloys $Ti_{47.5}Zr_{30}Mn_{15.5}V_5Ho_2$ and $Ti_{42.39}Zr_{27.34}Mn_{20.51}V_{6.86}Ho_2$, active hydrogen absorption started at 470°C, and the amounts of absorbed hydrogen H/Me equaled ~ 1.71 and 1.60, respectively (Fig. 4, *c*, *d*). When the holmium content increased to 5 at.%, the temperature of the absorption beginning raised up to 530°C. The amounts of absorbed hydrogen H/Me were ~ 1.69 and 1.58 for the alloys $Ti_{47.5}Zr_{30}Mn_{12.5}V_5Ho_5$ and $Ti_{41.97}Zr_{26.5}Mn_{19.88}V_{6.65}Ho_5$, respectively (Fig. 4, *e*, *f*).

As seen from Figure 4, the process of hydrogen absorption for all alloys at elevated temperatures has a similar nature and consists of two stages with noticeably different rates of interaction. The data of [4, 10] allow to suggest that the first stage of interaction with hydrogen corresponds to the formation of a supersaturated solid solution, whereas the second is the formation of the hydride phase.

It was previously shown that the process of hydrogen absorption in alloys with a two-phase structure (Laves phase and b.c.c. solid solution)

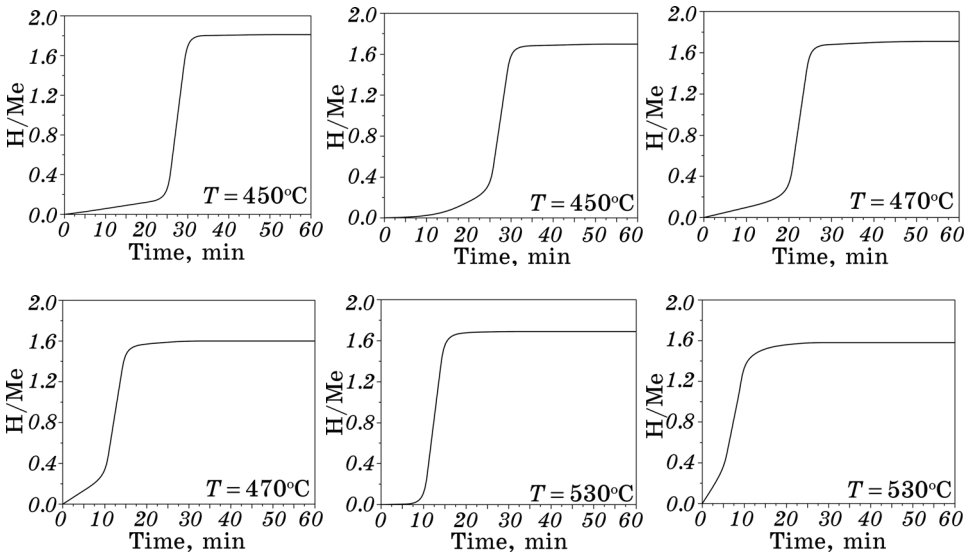

Fig. 4. Time curves of saturation of alloys with hydrogen under isothermal exposure at a hydrogen pressure of 0.6 MPa: $Ti_{47.5}Zr_{30}Mn_{17.5}V_5$ [20] (*a*), $Ti_{44.18}Zr_{27.9}Mn_{20.93}V_7$ [28] (*b*), $Ti_{47.5}Zr_{30}Mn_{15.5}V_5Ho_2$ (*c*), $Ti_{42.39}Zr_{27.34}Mn_{20.51}V_{6.86}Ho_2$ (*d*), $Ti_{47.5}Zr_{30}Mn_{12.5}V_5Ho_5$ (*e*), $Ti_{41.97}Zr_{26.5}Mn_{19.88}V_{6.65}Ho_5$ (*f*).

begins at room temperature on the crystallites of the Laves phase [33]. The coarsening of the phase constituents enhances the length of interphase boundaries and promotes hydrogenation, as it increases the mismatch of bulk expansion between neighbouring crystallites of two phases at the initial stages of hydrogenation, which causes higher stresses and surface cracking [33], activating hydrogen absorption. However, in the alloys with holmium (Table 1), despite the rather large surface area of the Laves phase crystallites, the absorption of hydrogen at room temperature did not occur, that can be explained by the formation of a new phase, holmium oxide (Fig. 1, *c*). It can be assumed that, in addition to clearly revealed coarse precipitates of the oxide phase (Fig. 1, *c*), a thin oxide film not visible by scanning electron microscopy formed on other surfaces of the phase constituents (Laves phase and b.c.c. solid solution). Holmium oxide film on the surface of Laves phase crystallites reduces their catalytic ability by lowering the active area for the dissociation of hydrogen molecules, forming a barrier layer that prevents the penetration of hydrogen into the lattice at room temperature.

The increment of holmium content, and accordingly its oxide volume fraction, enhance the barrier effect of the oxide film, so higher temperatures are required to activate the process of interaction with hydrogen. Nevertheless, the ratio of total amount of absorbed hydrogen to the fraction of Laves phase and b.c.c. solid solution was calculated by ImageJ software, and the results allow to suggest that the hydrogen capacity of these phases persisted virtually unchanged; therefore, the hydrogen content in the alloy remained proportional to the volume fraction of Laves phase and b.c.c. solid solution.

Beside holmium oxide which precipitated in the bulk of the alloy, an additional barrier to hydrogenation at room temperature was formed by the film of TiO_2 type which is always present on the surface of titanium alloys. As the temperature increases, this surface film gradually breaks down, and its barrier effect decreases due to the enhanced mobility of atoms in the lattice, that makes it possible to hydrogenate Ho-containing alloys at 470°C.

XRD phase analysis showed that the saturation of the alloys with hydrogen did not cause the decomposition of the phases or the formation of new phases, except the hydrides based on initial phases (Fig. 5, Table 3). The hydrogenation product obtained by saturating the investigated alloys of the Ti–Zr–Mn–V–Ho system with hydrogen comprised a hydride based on the Laves phase, δ-hydride, and holmium oxide. In addition to these phases, traces of holmium hydride of stoichiometric composition HoH_3 were also detected.

A comparison of the lattice parameters of holmium oxide (Table 3) shows that the parameter significantly increased after hydrogenation as compared to the initial state. It can be assumed that this increase

occurred because during heating holmium additionally absorbed oxygen atoms from the surface (in oxide films) and/or from the bulk of the material. The formed oxide phase absorbed additional oxygen atoms and gradually reached the stoichiometry composition Ho_2O_3 stable for this system. This property of holmium to bind oxygen present in the alloy potentially should improve the hydrogen absorption properties by reducing the amount of oxygen dissolved in the lattice, and so freeing the internodes for hydrogen atoms. The placement of one oxygen atom (which is 16 times larger than a hydrogen atom) in an internode leads to distortion of neighbouring internodes in each crystallographic direction [34], preventing the dissolution of hydrogen and reducing the total amount of absorbed hydrogen.

Mass-spectrometry of the hydrogenated alloys of Ti–Zr–Mn–V–Ho system under heating in vacuum showed that the entire process of hydrogen desorption from the Ho-containing alloys slightly shifted to higher temperatures in comparison with alloys without holmium [20]. At an initial pressure of $4 \cdot 10^{-3}$ Pa, hydrogen desorption in the hydrogenated alloys of the Ti–Zr–Mn–V–Ho system started at 80 ± 5°C (Fig. 6) which was 25°C higher compared to the alloys without holmium. Two peaks of gas desorption were observed: at 320°C (hydrogen desorption from hydride based on intermetallics), and at 370°C (hydrogen desorption from δ-hydride formed on the base of b.c.c. solid solution); in alloys without holmium, these temperatures were 265 and 390°C, respectively [20]. The calculations of areas under desorption curves showed that in the alloys of the Ti–Zr–Mn–V–Ho system 98–99% of hydrogen are desorbed at 550°C, whereas for the alloys without holmium the

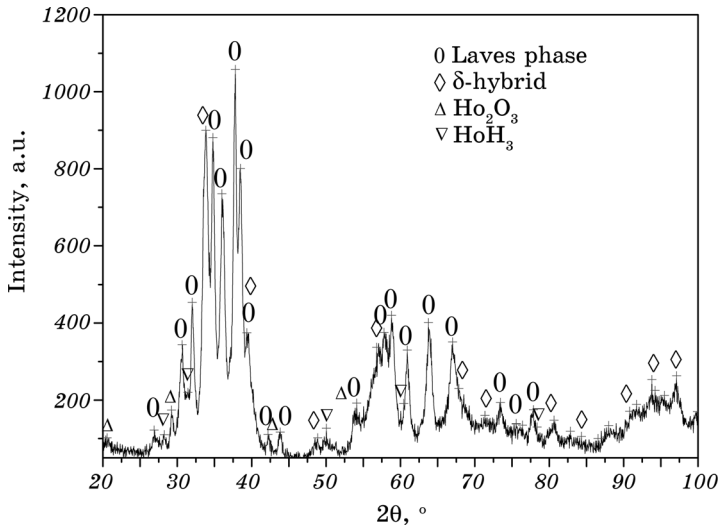

Fig. 5. Diffractogram of hydrogenated $Ti_{47.5}Zr_{30}Mn_{15.5}V_5Ho_2$ alloy.

corresponding temperature was 480°C [20, 28]. This delay in gas desorption in the alloys of the Ti–Zr–Mn–V–Ho system can also be explained by Ho_2O_3 precipitates and scale, that formed a barrier and delayed hydrogen diffusion from other phases to the surface.

The results of SEM, EDX, XRD phase analysis, and hydrogen sorption–desorption curves allow to adjust the previously determined pattern of the choice of alloying elements. When choosing an additional alloying element, it is necessary to take into account not only its atomic radius and ability to form a stable chemical compound with hydrogen, but also the mutual solubility with the main components of the alloy.

The above results allow to claim that the addition of holmium which is practically insoluble in the Laves phase and b.c.c. solid solution, alongside with other positive features of this alloying element, leads to both deterioration of hydrogen absorption properties (temperatures of hydrogen sorption–desorption) and reduction in the total amount of hydrogen absorbed. First, holmium is not soluble in the phase constituents of the alloys, it does not increase the lattice volume, and so it does not promote hydrogen absorption. Second, the total amount of absorbed hydrogen even decreases because holmium oxide precipitates in the alloy (in our experiments its volume fraction was 7.74–10.83%), which does not interact with hydrogen, and at the same time makes a significant contribution to the total weight of the material. And third, the hydrogen absorption conditions deteriorate because holmium oxide precipitates on the surface of Laves phase crystallites and b.c.c. solid solution, reduces the catalytic effect of the surface, and forms additional barrier

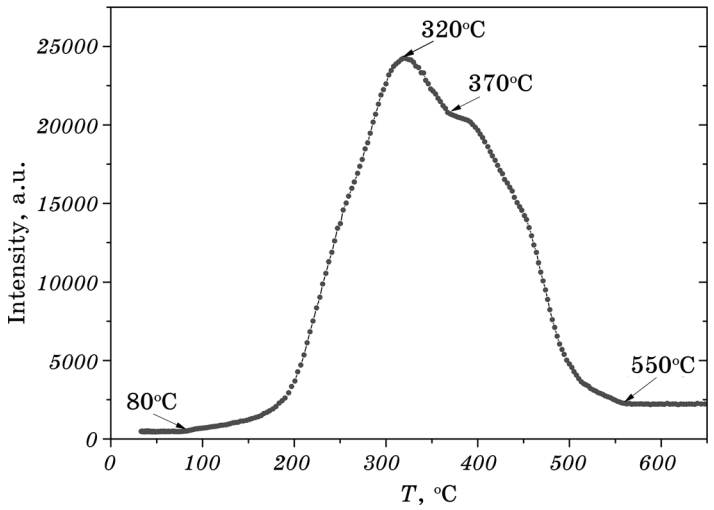

Fig. 6. Intensity of hydrogen desorption *vs.* temperature under continuous heating.

to the redistribution of hydrogen in the volume. Along with these factors, it is also important to consider the cost of holmium.

4. CONCLUSIONS

1. When choosing alloying elements to increase the hydrogen capacity of hydrogen-accumulating alloys, such an important factor as a high mutual solubility of these elements with the main components of the alloy, in addition to the atomic radius of the element and the ability to form a stable chemical compound with hydrogen. Low mutual solubility, and so the formation of new phases can deteriorate hydrogen capacity.
2. With regard to holmium alloying of the alloys of the Ti–Zr–Mn–V system, the insufficient solubility of this element and its high affinity for oxygen lead to the formation of new oxide phases, that is accompanied by a decrease in hydrogen capacity and deterioration of process kinetics during the first hydrogenation and desorption of hydrogen.

REFERENCES

1. M. B. Ley, L. H. Jepsen, Y. S. Lee, Y. W. Cho, J. Bellosta von Colbe, M. M. Dornheim, M. Rokni, J. O. Jensen, M. Sloth, Y. Filinchuk, J. E. Jørgensen, F. Besenbacher, and T. R. Jensen, *Mater. Today*, **17**: 122 (2014).
2. M. V. Lototskyy, *Int. J. Hydrogen Energy*, **41**: 2739 (2016).
3. D. Parra, M. Gillott, and G. S. Walker, *Int. J. Hydrogen Energy*, **41**: 5215 (2016).
4. K. T. Mollera, T. R. Jensena, E. Akiba, and H.-W. Li, *Prog. Nat. Sci.: Mat. Int.*, **27**: 34 (2017).
5. J. Bellosta von Colbe, J.-R. Ares, J. Barale, M. Baricco, C. Buckley, G. Capurso, N. Gallandat, D. M. Grant, M. N. Guzik, I. Jacob, E. H. Jensen, T. Jensen, J. Jepsen, T. Klassen, M. V. Lototskyy, K. Manickam, A. Montone, J. Puszkiel, S. Sartori, D. A. Sheppard, A. Stuart, G. Walker, C. J. Webb, H. Yang, V. Yartys, A. Züttel, and M. Dornheim, *Int. J. Hydrogen Energy*, **44**: 7780 (2019).
6. J. G. Park, H. Y. Jang, S. C. Han, P. S. Lee, and J. Y. Lee, *Mat. Sci. Eng. A*, **329–331**: 351 (2002).
7. E. I. Gkanas, M. Khzouz, G. Panagakos, T. Statheros, G. Mihalakakou, G. I. Siasos, G. Skodras, and S. S. Makridis, *Energy*, **142**: 518 (2018).
8. M. Lototskyy, I. Tolj, Y. Klochko, M. W. Davids, D. Swanepoel, and V. Linkov, *Int. J. Hydrogen Energy*, **45**: 7958 (2020).
9. T. R. Somo, M. W. Davids, M. V. Lototskyy, M. J. Hato, and K. D. Modibane, *Materials*, **14**: 1833 (2021).
10. V. A. Dekhtyarenko, D. G. Savvakin, V. I. Bondarchuk, V. M. Shyvanyuk, T. V. Pryadko, and O. O. Stasiuk, *Prog. Phys. Met.*, **22**: 307 (2021).
11. J. L. Bobet and T. B. Darriet, *Int. J. Hydrogen Energy*, **25**: 767 (2000).
12. S. Samboshi, N. Masahashi, and S. Hanada, *Acta Mater.*, **49**: 927 (2001).
13. S. Samboshi, N. Masahashi, and S. Hanada, *J. Alloys Compds.*, **352**: 210 (2003).

14. X. Y. Song, Y. Chen, Z. Zhang, Y. Q. Lei, X. B. Zhang, and Q. D. Wang, *Int. J. Hydrogen Energy*, **25**: 649 (2000).
15. N. Bouaziz, M. Bouzid, and A. B. Lamine, *Int. J. Hydrogen Energy*, **43**: 1615 (2018).
16. T. Huang, Z. Wu, G. Sun, and N. Xu, *Intermetallics*, **15**: 593 (2007).
17. P. Liu, X. Xie, L. Xu, X. Li, and T. Liu, *Prog. Nat. Sci.: Mat. Int.*, **27**: 652 (2017).
18. N. N. Greenwood and A. Earnshaw, *Chemistry of the Elements* (Oxford: Butterworth Heinemann: 1997).
19. Z. Yao, L. Liu, X. Xiao, C. Wang, L. Jiang, and L. Chen, *J. Alloys Compds.*, **731**: 524 (2018).
20. V. G. Ivanchenko, V. A. Dekhtyarenko, and T. V. Pryadko, *Metallofiz. Noveishie Tekhnol.*, **37**, No. 4: 521 (2015).
21. T. V. Pryadko, V. A. Dekhtyarenko, K. M. Khranovs'ka, and H. S. Mohyl'nyi, *Mater. Sci.*, **55**: 854 (2020).
22. I. Jacob, A. Stern, A. Moran, D. Shaltiel, and D. Davidov, *J. Less-Common Met.*, **73**: 369 (1980).
23. H. Taizhong, W. Zhu, Y. Xuebin, C. Jinzhou, X. Baojia, H. Tiesheng, and X. Naixin, *Intermetallics*, **12**: 91 (2004).
24. J. A. Murshidi, M. Paskevicius, D. A. Sheppard, and C. E. Buckley, *Int. J. Hydrogen Energy*, **36**, Iss. 13: 7587 (2011).
25. K. Young, T. Ouchi, J. Nei, and T. Meng, *J. Power Sources*, **281**: 164 (2015).
26. S. Khajavi, M. Rajabi, and J. Huot, *J. Alloys Compds.*, **767**: 432 (2018).
27. V. G. Ivanchenko, V. A. Dekhtyarenko, T. V. Pryadko, and V. I. Nichiporenko, *Metallofiz. Noveishie Tekhnol.*, **36**, No. 6: 803 (2014) (in Russian).
28. V. A. Dekhtyarenko, T. V. Pryadko, D. G. Savvakin, and T. A. Kosorukova, *Metallofiz. Noveishie Tekhnol.*, **41**, No. 11: 1455 (2019) (in Russian).
29. G. F. Kobzenko and A. A. Shkola, *Mater. Diagnos.*, **56**: 41 (1990) (in Russian).
30. J. R. Johnson, *J. Less-Common Met.*, **73**: 345 (1980).
31. J. Bodega, J. F. Fernández, F. Leardini, J. R. Ares, and C. Sánchez, *J. Phys. Chem. Solids*, **72**: 1334 (2011).
32. V. G. Ivanchenko, V. A. Dekhtyarenko, T. V. Pryadko, D. G. Savvakin, and I. K. Evlash, *Mater. Sci.*, **51**: 492 (2016).
33. V. A. Dekhtyarenko, T. V. Pryadko, D. G. Savvakin, V. I. Bondarchuk, and G. S. Mogylnyy, *Int. J. Hydrogen Energy*, **46**: 8040 (2021).
34. J. G. Niu and W. T. Geng, *Acta Mater.*, **81**: 194 (2014).